PHYSICAL REVIEW B VOLUME 25, NUMBER 10 15 MAY 1982

Physics of lattice relaxation at surfaces of simple metals

J. P. Perdew
Department of Physics and Quantum Theory Group, Tulane University, New Orleans, Louisiana 70118
(Received 30 June 1981)

The physics of the inward or outward relaxation of the first plane of ions at a metal surface is explored by means of semi-self-consistent calculations for Al, Mg, and Na. The adiabatic screening response of the electron density to a shift of the first lattice plane drastically reduces the curvature of the potential in which this plane sits, and thus cannot be ignored in any qualitatively correct theory of the equilibrium lattice configuration at the surface. Because the electronic screening is nearly perfect, the calculated face-dependent surface energies and work functions are nearly independent of small displacements of the first lattice plane. Just as in the calculation of the bulk-longitudinal-phonon frequencies, there is a delicate cancellation between Madelung forces which are treated exactly and electronic forces which are approximated. Indeed a quantitatively correct theory of the surface interplanar spacing must also be detailed enough to predict the correct bulk-phonon frequencies.

I. INTRODUCTION

The first few lattice planes of ions at a metal surface can relax inward or outward. For example, the first interplanar spacing at the aluminum (111) surface appears to be 2% greater than the bulk spacing according to low-energy electron diffraction (LEED) measurements[1] [or 8% smaller according to extended x-ray absorption fine structure[2] (EXAFS)]. This spacing is calculable in principle by direct minimization of the surface energy.

We present here a simple variational calculation of surface lattice relaxation in Al, Mg, and Na. Some of the results for Al were presented in an earlier Letter.[3] The calculation is not detailed enough to predict lattice spacings accurately, but it is sufficiently realistic to answer some questions about the basic physics: (1) Which forces drive the first lattice plane inward, and which outward? (2) How important is the screening response of the electron density to displacements of the first lattice plane? (3) How strongly are surface energies and work functions affected by lattice relaxation? (4) What conditions are necessary for a calculation of surface interplanar spacing to be qualitatively or quantitatively correct?

II. DESCRIPTION OF THE MODEL

A. Energy functional

Bulk and surface energies of metals can be divided into classical Madelung and electronic contributions. The Madelung term is the electrostatic energy of point ions neutralized by a uniform, semi-infinite negative background filling the half-space $x<0$. It is always treated exactly. The layer-summation method[4-7] was used to derive expressions for the Madelung or classical cleavage contribution to the surface energy, including relaxation of the first lattice plane (Appendix A). These expressions were also derived independently by another group.[6]

The electronic energy includes the energy of a semi-infinite jellium plus discrete-lattice corrections. The jellium is a system of valence electrons neutralized by a uniform positive background filling the half-space $x<0$. Its energy functional includes kinetic, electrostatic, and exchange-correlation terms. The jellium surface is transformed into the real-metal surface by turning on an "external" potential $\delta v(r)$, the discrete-lattice potential, which is the difference beween the pseudopotentials of the semi-infinite lattice and the electrostatic potential of the semi-infinite uniform positive background. The electron density and energy are constructed from orbitals which are the eigenfunctions of a self-consistent one-electron Hamiltonian. Detailed expressions for the energy functional have been given elsewhere.[8]

As in Ref. 8, we use the standard Ashcroft empty-core pseudopotential. The pseudopotential core radii r_c are given in Table I, which also displays the valence, crystal structure, and average bulk electron density $\bar{n}=(4\pi r_s^3/3)^{-1}$ a.u. Ex-

TABLE I. Inputs to the calculation are the valence z, crystal structure, and bulk interelectron separation r_s. The Ashcroft pseudopotential core radius r_c is chosen to make the calculated bulk-binding energy per electron ϵ minimize at the observed value of r_s. ϵ^{theor}, the value of ϵ at the minimum, is in good agreement with the experimental bulk-binding energy ϵ^{expt}. (For hcp Mg, $c/a=1.625$.)

Metal	z	Structure	r_s	r_c	ϵ^{theor}	ϵ^{expt}
			(a.u.)		(eV)	
Al	3	fcc	2.07	1.12	−18.9	−18.8
Mg	2	hcp	2.65	1.31	−12.3	−12.1
Na	1	bcc	3.99	1.75	−6.3	−6.3

change and correlation are treated in the local density approximation, using a parametrization[9] of the accurate electron-gas correlation energies of Ceperley and Alder. A nonlocal correction of (1300 erg/cm^2)/r_s^3 has also been included in the surface exchange-correlation energy. This expression, which depends only on the bulk density $\bar{n}$ and not on the surface density profile, summarizes the results of the density-fluctuation wave-vector interpolation method.[10]

As a test of the energy functional, the *bulk* longitudinal-phonon frequencies of aluminum (Fig. 1) have been calculated, using the standard expression[11] to second order in the pseudopotential. The Madelung energy, which is treated exactly, leads to phonon frequenices much higher than experiment.[11] The electronic energy is treated approximately (Ashcroft pseudopotential, local density exchange correlation), and the approximation satisfactorily cancels most of the Madelung contribution to the phonon frequencies, especially at long wavelengths (perfect screening). However, the phonon frequencies themselves, which are the residue of this delicate cancellation, are not spectacularly accurate in comparison with experiment.

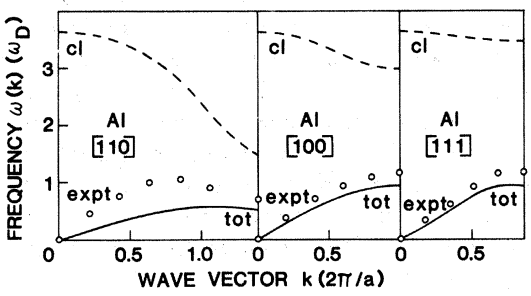

FIG. 1. Bulk-longitudinal-phonon frequencies of Al, expressed in units of the Debye frequency $\omega_D=5.16\times10^{13}$ rad/sec ($\Theta_D=394$ K). Dashed curves; calculated using classical Madelung forces only (Ref. 11). Solid curves: calculated using Madelung plus electronic forces (Ashcroft pseudopotential, local density approximation). Open circles: experiment (Ref. 11). a is the lattice constant. The unpublished experimental results cited in Ref. 11 were later published in Ref. 25.

B. Model density profile

The assumed position of the first lattice plane is

$$x_\lambda=(-\tfrac{1}{2}+\lambda)d\ , \tag{1}$$

where d is the bulk interplanar spacing and $\lambda=0$ for the unrelaxed lattice. For each choice of λ we calculate the surface energy by substituting into the energy functional the self-consistent electron density profile of a jellium surface (with uniform positive background filling the half-space $x<0$) perturbed by an external potential V_λ. If V_λ were the discrete-lattice potential $\delta v_\lambda(\vec{r})$, our calculation would be fully self-consistent but difficult because of the three-dimensional variation of the resulting

TABLE II. $\langle\delta v_0\rangle_{\text{av}}$ is the average of the discrete-lattice potential over the volume of the semi-infinite system, and C is the variational parameter of Eq. (2), for an unrelaxed surface.

Metal	Face	$\langle\delta v_0\rangle_{\text{av}}$ (eV)	C
Al	(111)	−1.7	−1.9
	(100)	0.2	1.0
	(110)	3.0	3.6
Mg	(0001)	−0.7	−0.4
Na	(110)	0.2	0.6
	(100)	1.1	1.3
	(111)	1.7	1.6

electron density. We use instead the one-dimensional potential

$$V_\lambda(x)=C\Theta(-x)+\delta v_\lambda(x)-\delta v_0(x)\ , \tag{2}$$

where $\Theta(-x)$ is a step function which vanishes outside the jellium surface and $\delta v_\lambda(x)$ is the planar average of $\delta v_\lambda(\vec{r})$. The constant C is chosen to minimize the surface energy of the unrelaxed system, and mimics $\langle \delta v_0 \rangle_{\rm av}$, the average of $\delta v_0(\vec{r})$ over the volume of this semi-infinite system. We checked that the minimizing value of C was nearly independent of λ, in agreement with our physical interpretation of it, and we have used the value for $\lambda=0$ (Table II) in the calculations presented here.

This model has been used with some success in our earlier calculations[8,12] of the surface energy, electron density, and work function of the unrelaxed surface. It yields a one-dimensional density profile $n(x)$, varying only in the direction perpendicular to the surface and tending to a constant $\bar{n}$ in the bulk, which has a *realistic* surface dipole moment

$$\int_{-\infty}^{\infty} dx\, 4\pi e^2 x[n(x)-\bar{n}\Theta(-x)] \tag{3}$$

(where the step function $\Theta(y)$ equals 1 for positive y and 0 for negative y). This is shown by a comparison[12] of measured work functions with work functions calculated from the profile-sensitive Koopmans-theorem expression, and by some more direct experimental evidence.[13] The choice $C=0$ in Eq. (2) would deliver the density profile of the unperturbed jellium surface, which usually does *not* have a realistic dipole moment; this choice would reduce our model to the one used in the pioneering surface calculations of Lang and Kohn.[14]

For the relaxed surface, Eq. (2) includes the ionic relaxation dipole. We have used the general expression for $\delta v_\lambda(x)$ described in Appendix A. For small displacements of the first lattice plane ($|\lambda| << 1$), this expression reduces to the simple result

$$\delta v_\lambda(x)-\delta v_0(x)=\begin{cases} 0 & (x > -\frac{1}{2}d+r_c) \\ 2\pi e^2\bar{n}d^2\lambda & (-\frac{1}{2}d-r_c<x<-\frac{1}{2}d+r_c) \\ 4\pi e^2\bar{n}d^2\lambda & (x<-\frac{1}{2}d-r_c)\ . \end{cases} \tag{4}$$

Thus an inward displacement ($\lambda<0$) steps down the potential twice: first at the outer edge of the ion cores of the first lattice plane, and next at the inner edge. The model allows the electron density to respond self-consistently to this perturbation.

Our model assumes that the electron density in the bulk is a constant $\bar{n}$. In order to avoid spurious relaxations at the surface, the pseudopotential core radius r_c (Table I) has been adjusted so that the bulk energy per electron, assuming a constant bulk density, minimizes at the observed density $\bar{n}$. For aluminum this procedure[15] just recovers the conventional value of r_c. The value of this energy at the minimum, the bulk binding energy, is in satisfactory agreement with experiment for all three metals (Table I).

In any calculation of lattice relaxation, an important quantity is the curvature of the potential in which the first lattice plane sits, i.e., the second derivative of the surface energy σ with respect to the displacement parameter λ. This curvature is essentially a spring constant

$$\frac{d^2\sigma}{d\lambda^2}=\frac{d^3}{\Omega_0}M\omega^2\ , \tag{5}$$

where Ω_0 is the volume per atom in the crystal, M is the mass of an ion, and ω is the frequency for small vibrations of the first lattice plane, with the other lattice planes clamped fast. A related quantity is the curvature of the potential or vibration frequency ω for a similar lattice plane in the *bulk*. The bulk ω^2 is just the average squared-longitudinal-phonon frequency for wave vectors $\vec{k}$ normal to the lattice plane of interest:

$$\omega^2=\frac{d}{\pi}\int_0^{\pi/d} dk\,\omega^2(k)\ , \tag{6}$$

as derived in Appendix B. Table III shows bulk values of ω^2 calculated in three ways: (1) from the classical Madelung approximation[11] to the phonon frequencies (Fig. 1), which ignores the screening response of the electrons to a lattice wave, (2) from the Madelung plus self-consistent electronic approximation (Fig. 1), and (3) from our model (Appendix B). Methods (2) and (3) employ the same energy functional, but (2) is fully self-consistent while (3) uses our model for the electron density in the bulk (uniform for a perfect lattice, with a self-consistent response to the planar average of the change in the discrete-lattice potential induced by a

TABLE III. ω^2/ω_D^2, a dimensionless measure of the curvature of the potential in which a *bulk* lattice plane sits, for three different lattice planes in aluminum. ω is the vibration frequency of one plane with the others clamped fast, and ω_D is the Debye frequency. The Madelung approximation ignores the screening response of the electrons, which is included either self-consistently (with three-dimensional density variations) or via our model (with one-dimensional density variations) in the other two calculations.

Bulk ω^2/ω_D^2	(111)	(100)	(110)
classical Madelung	12.7	11.2	8.7
total (self-consistent)	0.4	0.4	0.2
total (model)	0.0	0.2	0.9

lattice-plane displacement). Since there is little detailed agreement between methods (2) and (3), our model *cannot* be relied on for quantitiative prediction of surface lattice relaxation. However, methods (2) and (3) agree qualitatively—both exhibit a reduction of ω^2 due to electronic screening by about an order of magnitude from its Madelung value. Thus, our model is qualitatively correct: It exhibits the important physics of screening.

III. RESULTS

A. Surface energies

Figures 2—4 show the calculated surface energies σ as a function of the lattice displacement parameter λ. Na and Mg display the same behavior found earlier[3] for Al: The total surface energy $\sigma_{\rm tot}$ depends weakly on λ, although the individual components of it have a strong λ dependence.

The classical Madelung energy $\sigma_{\rm cl}$ shows a strong positive curvature $d^2\sigma_{\rm cl}/d\lambda^2$. $\sigma_{\rm cl}$ tends to drive the first lattice plane *inward* from its unrelaxed ($\lambda=0$) position. The minimum of $\sigma_{\rm cl}$ is close to $\lambda=0$ for the more densely packed crystal faces [fcc (111), bcc (110), and hcp (0001)], but lies substantially further inward for the more loosely packed faces. These exact results agree with earlier conclusions based on an approximation to $\sigma_{\rm cl}$.[16]

The strong positive curvature of $\sigma_{\rm cl}$ is mostly cancelled by the strong negative curvature of the electronic part of the surface energy, especially the pseudopotential part

$$\sigma_{\rm ps}=\int_{-\infty}^{\infty} dx[n(x)-\bar{n}\Theta(-x)]\delta v_\lambda(x)\ . \qquad (7)$$

The curvatures of $\sigma_{\rm cl}$ and $\sigma_{\rm tot}$ are expressed in terms of ω^2 according to Eq. (5) in Table IV. The same delicate cancellation due to screening was

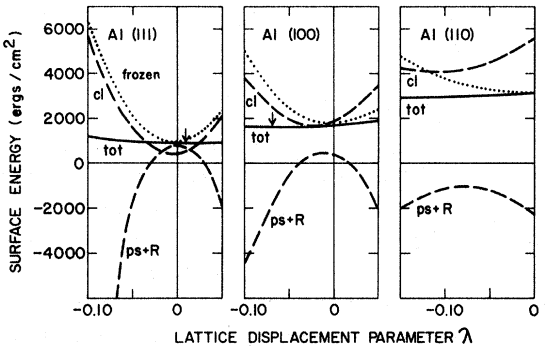

FIG. 2. Variation of the calculated total surface energy for Al (solid curves) with displacement of the first lattice plane. Minima are indicated by downward-pointing arrows. The classical cleavage (cl) or Madelung and the pseudopotential plus repulsive (ps + R) components of the total are shown as dashed curves; for clarity the kinetic, electrostatic and exchange-correlation components are not shown. The dotted curve is the total surface energy evaluated with a "frozen" electron density profile (the one for $\lambda=0$).

found earlier in the bulk (Table III). Comparison of Tables III and IV suggests that the first lattice plane at the surface may have a higher vibration frequency ω, and smaller zero-point motion than a similar plane in the bulk, but this result could be an artifact of the model.

The slopes $d\sigma/d\lambda$ of $\sigma_{\rm cl}$ and $\sigma_{\rm ps}$ also tend to cancel. The pseudopotential energy $\sigma_{\rm ps}$ usually drives the first lattice plane *outward* from its unrelaxed position. This result is easily understood:

Let $n(\vec{r})$ and $\sigma_{\rm tot}$ be the *self-consistent* electron density and surface energy. The force per unit area on the first lattice plane at position x_λ, $-d\sigma_{\rm tot}/dx_\lambda$, is given by the generalized Hellmann-Feynman theorem[17]:

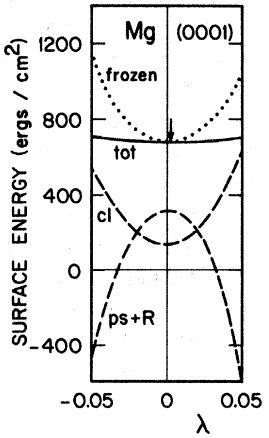

FIG. 3 Same as Fig. 2 for Mg.

$$-\frac{d}{dx_\lambda}\sigma_{\rm tot}=-\frac{d}{dx_\lambda}\sigma_{\rm cl}-\frac{d}{dx_\lambda}\sigma_R-\int_{-\infty}^{\infty}dx\left\langle[n(\vec{r})-\bar{n}\Theta(-x)]\frac{d}{dx_\lambda}\delta v_\lambda(\vec{r})\right\rangle , \tag{8}$$

where $\langle\ \rangle$ indicates a planar average. The "repulsive" energy[8]

$$\sigma_R=-\pi e^2\bar{n}^2 d(r_c+x_\lambda)^2\Theta(r_c+x_\lambda) \tag{9}$$

is zero as long as the ion cores are confined to the half space $x<0$, which is usually the case. The last term in Eq. (8) becomes in our model

$$-\int_{-\infty}^{\infty}dx[n(x)-\bar{n}\Theta(-x)]\frac{d}{dx_\lambda}\delta v_\lambda(x)\approx -2\pi e^2\bar{n}d\int_{-d/2-r_c}^{-d/2+r_c}dx\,[n(x)-\bar{n}] -4\pi e^2\bar{n}d\int_{-\infty}^{-d/2-r_c}dx[n(x)-\bar{n}] , \tag{10}$$

where the right-hand side was obtained using Eq. (4). (We are using the Hellmann-Feynman theorem only for discussion, not for calculation.) The first term on the right-hand side of Eq. (10) is usually an *outward* force (for all λ of interest) because there is a deficiency of electrons over the first layer of cores (Fig. 5). The second term is usually negligible for $\lambda=0$ because the density is bulk-like behind the first layer of cores. For $\lambda<0$, the electron density builds up behind the first layer of cores (Fig. 5), and this term becomes an inward force which for very negative λ cancels most of the outward force from the classical Madelung energy.

The surface energies calculated for Al, unlike those calculated for Na, are strongly face dependent, being about three times greater for the (110) face than for the more close-packed (111) face. The large surface energies calculated for the more open faces of Al conflict both with experiment[18] and with a recent calculation.[19] The latter suggests that they are an artifact of the one-dimensional approximation for the electron density. Certainly these anomalously large surface energies cannot be corrected by lattice relaxation.

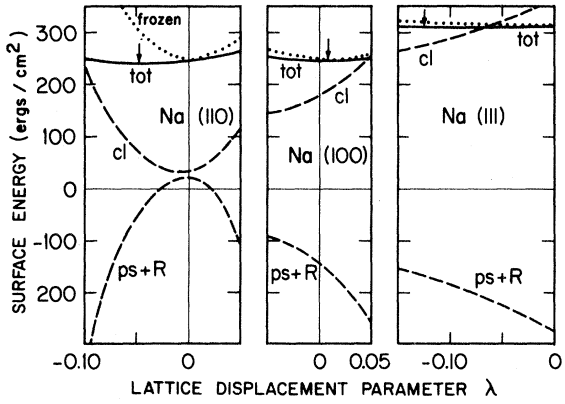

FIG. 4 Same as Fig. 2 for Na.

Figures 2–4 also show the λ dependence of the total surface energy which would be predicted by the "frozen-profile" approximation,[4,7,14,16] which allows no electron density response to the shift of the first lattice plane. Because this approximation neglects screening, it grossly exaggerates the curvature of the potential in which the first lattice plane sits.

B. Electron density profiles

Figure 5 compares the electron density profile for the unrelaxed surface to that for a hypothetical inward displacement of the first lattice plane by 5% of the bulk interplanar spacing, for three faces of Al. The screening response of the electron density is greatest for the (111) face, for two reasons: This plane has the highest density of ions and also moves farthest in a 5% contraction.

Figure 5 also shows the positions and sizes of the ion cores in the unrelaxed lattice. The screening response of the electron density to an inward displacement of the first lattice plane is simply to transfer electron density from in front of to behind

TABLE IV. ω^2/ω_D^2, a dimensionless measure of the curvature of the potential in which the first lattice plane sits, at three different *surfaces* of aluminum. ω is the vibrational frequency of this plane with the others clamped fast, and ω_D is the Debye frequency. The Madelung approximation ignores the screening response of the electrons, which is included approximately in our model.

Surface ω^2/ω_D^2	(111)	(100)	(110)
classical Madelung	13.0	12.2	11.0
total (model)	0.6	0.8	1.2

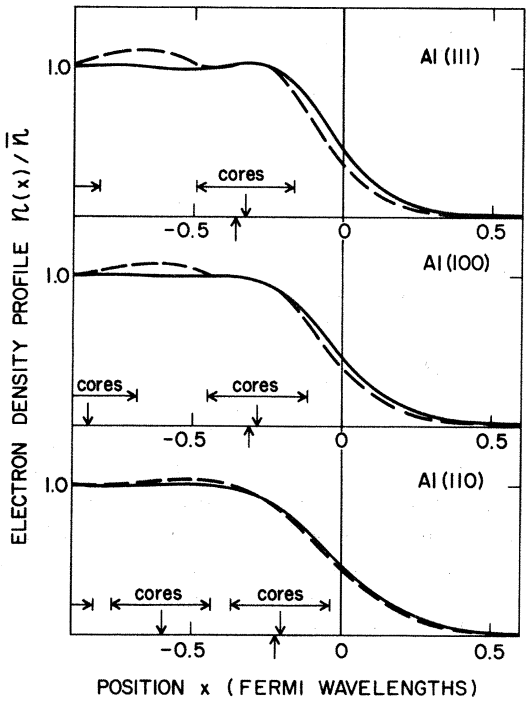

FIG. 5. Calculated electron density profiles for three Al surfaces. The solid curves are for the unrelaxed lattice, with the position of the first lattice plane indicated by a downward-pointing arrow. The dashed curves are for a hypothetical inward relaxation of the first lattice plane, by 5% of the bulk interplanar spacing, to a position indicated by an upward-pointing arrow; note the heaping up of electronic charge behind the cores of the displaced lattice plane.

the first layer of ion cores. In an earlier Letter,[3] we showed how similar this is, both qualitatively and quantitatively, to the linear response of a *uniform* electron gas to the perturbation Eq. (4).

C. Work functions

Within a restricted variational calculation such as this one, work functions W can be calculated most accurately by the "change-in-self-consistent-field" (ΔSCF) expression[12]:

$$W^{\Delta\mathrm{SCF}}=\left.\frac{d\sigma_{\mathrm{tot}}}{d\Sigma}\right|_{\Sigma=0}, \tag{11}$$

where Σ is the surface charge density. A simplified version of Eq. (11) has been used to calculate work functions for many simple metals, neglecting lattice relaxation.[20]

Table V shows work functions calculated from the full expression Eq. (11) for the unrelaxed surface and for an assumed 5% contraction of the first interplanar spacing. Within the numerical accuracy of the calculation, the work function is found to be independent of the lattice displacement parameter λ, in accord with theoretical expectations.[8] Thus, the screening of the ionic relaxation dipole by the electrons is essentially perfect. But if the electron density were "frozen" so that it could not respond to the shift of the first lattice plane, the work function would depend *strongly* on λ,

$$W_{\lambda}^{\mathrm{frozen}}=W_{0}^{\Delta\mathrm{SCF}}+\langle\delta v_{0}\rangle_{\mathrm{av}}-\langle\delta v_{\lambda}\rangle_{\mathrm{av}}, \tag{12}$$

as shown in Table V.

TABLE V. Face-dependent work functions calculated from the ΔSCF expression Eq. (11), for the unrelaxed ($\lambda=0$) surface and for a hypothetical inward displacement of the first lattice plane by 5% of the bulk interplanar spacing ($\lambda=-0.05$). The last column shows what the work function for $\lambda=-0.05$ would be if the electron density profile were "frozen," Eq. (12).

Metal	Face	$W_0^{\Delta\mathrm{SCF}}$	$W_{-0.05}^{\Delta\mathrm{SCF}}$	$W_{-0.05}^{\mathrm{frozen}}$
			(eV)	
Al	(111)	4.2	4.1	13.1
	(100)	4.1	4.1	7.9
	(110)	3.7	3.7	7.1
Mg	(0001)	3.9	4.0	9.2
Na	(110)	2.9	2.9	5.0
	(100)	2.7	2.7	3.7
	(111)	2.6	2.6	2.9

IV. CONCLUSIONS

We can now answer the questions raised in the Introduction:

(1) When the first lattice plane sites at its unrelaxed position, classical Madelung forces tend to drive it inward while electronic forces, especially those arising from the pseudopotential energy Eq. (7), usually tend to drive it outward. These results agree with those of other calculations.[6,7] When the first lattice plane is displaced far enough inward, these forces each reverse direction. For most displacements of interest, there is a strong cancellation between Madelung and electronic forces.

(2) Of course the "initial forces of relaxation" acting on the unrelaxed first lattice plane can be

calculated neglecting the adiabatic screening response of the electron density to a shift of the first lattice plane, according to the Hellmann-Feynman theorem Eq. (8). However, the screening response of the electron density drastically reduces the first derivative of the force (second derivative of the surface energy $\sigma_{\rm tot}$) with respect to displacement of the first lattice plane. Hence screening *crucially* affects the equilibrium lattice configuration at the surface.

(3) Because the electronic screening is nearly perfect, surface energies and work functions are almost independent of small displacements of the first lattice plane. Calculations of these quantities which assume an unrelaxed lattice should not be affected by lattice relaxation.

(4) A *qualitatively* correct calculation of lattice relaxation should include the screening response of the electron density to displacements of the first lattice plane. Calculations in which the electron density profile is "frozen"[4,7,14,16] have omitted some qualitatively important physics, although they have also contributed to our understanding of the problem. (Of course, the authors of most of these calculations acknowledged the possible importance of the omitted physics of "screening.") The same may be said of calculations which allow the electrons to respond to a shift of the first lattice plane only in a limited way,[6,8,15] which does not permit wholesale transfer of electrons across the first layer of cores as in Fig. 5. For example, in a early calculation[8] for Al we used not Eq. (2) but $V_\lambda(x)=C_\lambda\Theta(-x)$, where C_λ was found by minimization of the surface energy for each λ. Like the "frozen-profile" method, this approach grossly exaggerates the curvature of the potential in which the first lattice plane sits. Only a few previous calculations[3,17] seem to have allowed for the right qualitative screening.

A *quantitatively* correct calculation of interplanar spacings at the surface of a simple metal must meet some very stringent conditions:

(a) It must include the variation of the electron density in three dimensions, not just one. Such calculations[19,21] have only recently been carried out for the surface energy of the *unrelaxed* lattice. Within the context of the present calculation, we would have to re-introduce $\delta v_\lambda(\vec{r})-V_\lambda(x)$ as a weak perturbation on our solution, carrying the density to first order and the energy to second order. If the half-space $x<0$ is divided up into prismatic unit cells around each ion, the main effect of $\delta v_\lambda(\vec{r})-V_\lambda(x)$ should be to redistribute the electron density inside each cell, especially by driving electrons out of the cores and heaping them up just outside the cores. This may contribute an additional outward force on the first lattice plane, as suggested by the Hellmann-Feynman theorem, Eq. (8), and other arguments.[4,17] It may also modify the curvature of the potential in which the first lattice plane sits, as suggested by Table III.

(b) The energy functional and method of calculation, when applied to the bulk crystal, must predict *both* the measured equilibrium density *and* the measured phonon frequencies. The former condition is necessary for the correct initial slope of $\sigma_{\rm tot}$ versus λ, and the latter for the correct curvature. We have emphasized the latter condition here, since the former has been emphasized by others[4,16,22] who have pointed out that bulk pair potentials, which omit volume-dependent energies are inadequate for the surface relaxation problem.

(c) Multilayer relaxation was found to be important for some metal surfaces in a recent "frozen profile" calculation.[7] Since the screening response of the electrons should weaken *both* the disturbing and restoring forces on the second and third lattice planes, it remains to be seen if multilayer relaxation is also necessary for a quantitatively correct calculation.

Very recently there appeared a calculation[23] of lattice relaxation at sodium surfaces which properly allows for both electronic screening and three-dimensional electron density variation.

ACKNOWLEDGMENTS

I would like to thank Dr. René Monnier for his collaboration, and Eidgenössische Technische Hochschule—Zürich for its hospitality, during the earlier stages of this work. Part of this work was supported by the National Science Foundation Grant No. DMR80-16117.

APPENDIX A: RELAXATION CONTRIBUTIONS TO CLASSICAL CLEAVAGE ENERGY AND DISCRETE-LATTICE POTENTIAL

General expressions for the relaxation contribution to the classical cleavage energy $\sigma_{\rm cl}(\lambda)$ were derived and presented in Ref. 6. For all the surfaces considered here and for $-\frac{1}{2}<\lambda<\frac{1}{2}$, we have found the simpler result

$$\sigma_{cl}(\lambda)-\sigma_{cl}(0)=2\pi e^2\bar{n}^2d^3\left[\lambda^2+\sum_{m,n}{}'\frac{1}{\zeta_{mn}}\frac{S_{mn}(e^{-\lambda\zeta_{mn}}-1)}{e^{N\zeta_{mn}}-1}\right], \tag{A1}$$

where

$$S_{mn}=\sum_{k=1}^{N}e^{(k-1)\zeta_{mn}}\cos\left[\frac{2\pi}{N}(k-1)(m+n)\right]. \tag{A2}$$

Here d is the unrelaxed interplanar spacing, and Nd is the stacking period. The sum in Eq. (A1) ranges over all integers m and n except those for which $\zeta_{mn}=0$. ζ_{mn} is the product of d with the projection of a three-dimensional reciprocal-lattice vector onto the plane of the surface. Table VI shows all the relevant geo- metric information.

Finally, consider the planar-average discrete-lattice potential $\delta v_\lambda(x)$. Expressions for the unrelaxed potential $\delta v_0(x)$ have been given elsewhere.[8,14] The relaxation contribution $\delta v_\lambda(x)-\delta v_0(x)$ is the sum of two pieces. The first arises from point ions:

$$\begin{cases} 0 & (x\geq a), \\ 4\pi e^2\bar{n}d^2\lambda\dfrac{(a-x)}{(a-b)} & (b<x<a), \\ 4\pi e^2\bar{n}d^2\lambda & (x\leq b), \end{cases} \tag{A3}$$

where a and b are, respectively, the greater and lesser of the numbers $-\frac{1}{2}d$ and $(-\frac{1}{2}+\lambda)d$. The second piece, which arises from the short-range repulsion in the core, is

$$u_2(x-\lambda d)-u_2(x), \tag{A4}$$

where

$$u_2(x)=2\pi e^2\bar{n}d(r_c-|x+\tfrac{1}{2}d|)\Theta(r_c-|x+\tfrac{1}{2}d|). \tag{A5}$$

APPENDIX B: VIBRATION FREQUENCY OF ONE LATTICE PLANE IN THE BULK

Here we will calculate the vibration frequency ω of one lattice plane in a bulk crystal, with the other planes clamped fast. Let the lattice sites be specified by position vectors $\vec{l}$, and let $\hat{x}$ be the normal to the lattice plane of interest ($l_x=0$). Consider an infinitesimal displacement of this plane alone:

$$\vec{u}(\vec{l})=u\hat{x}\delta_{l_x,0}. \tag{B1}$$

The Kronecker delta may be constructed from plane waves in the first Brillouin zone (BZ):

$$\delta_{l_x,0}=\frac{1}{N_x}\sum_{k_x}^{BZ}e^{ik_xl_x}=\frac{d}{2\pi}\int_{-\pi/d}^{\pi/d}dk_xe^{ik_xl_x}, \tag{B2}$$

TABLE VI. Geometric information for the relaxation contribution to the classical cleavage energy. a and c are conventional lattice constants.

Structure	Face	N	d	ζ_{mn}
fcc	(111)	3	$\frac{a}{\sqrt{3}}$	$\frac{4\pi}{3}[2(m^2+n^2-mn)]^{1/2}$
	(100)	2	$\frac{a}{2}$	$\pi[2(m^2+n^2)]^{1/2}$
	(110)	2	$\frac{a}{2\sqrt{2}}$	$\frac{\pi}{2}[2(m^2+2n^2)]^{1/2}$
bcc	(110)	2	$\frac{a}{\sqrt{2}}$	$\pi[(m-n)^2+2(m+n)^2]^{1/2}$
	(100)	2	$\frac{a}{2}$	$\pi(m^2+n^2)^{1/2}$
	(111)	3	$\frac{a}{2\sqrt{3}}$	$\frac{\pi}{3}[2(m^2+n^2-mn)]^{1/2}$
hcp	(0001)	2	$\frac{c}{2}$	$\frac{\pi c}{a}[m^2+(m-2n)^{2/3}]^{1/2}$

where d is the distance between neighboring planes in the perfect crystal, and N_x is the number of such planes. The energy of this superposition of longitudinal phonons, divided by the number of ions in the plane, is just

$$\delta E = \frac{1}{N_x}\sum_{k_x}^{\mathrm{BZ}} \tfrac{1}{2} M\omega^2(k_x)u^2$$
$$= \tfrac{1}{2} Mu^2 \frac{d}{\pi}\int_0^{\pi/d} dk_x \omega^2(k_x) , \qquad \text{(B3)}$$

where $\omega(k_x)$ is the frequency of a longitudinal phonon of wave vector $k_x\hat{x}$, and M is the mass of an ion. But by definition

$$\delta E = \tfrac{1}{2} M\omega^2 u^2 . \qquad \text{(B4)}$$

Equations (B3) and (B4) imply Eq. (6), an exact result.

Now consider our *model* applied to this problem. For the perfect crystal, the electrons are assumed to have uniform density. The displacement, Eq. (B1), is assumed to produce an external perturbation $\Delta v(\vec{r})$ of the form of Eq. (4), with $\lambda = u/d$. [Without loss of generality, we will consider a lattice plane in the center of a crystal, and add the constant $-2\pi e^2 \bar{n} d^2 \lambda$ to Eq. (4) in order to have a perturbation of zero average value.] The resulting change in the electronic energy of the crystal (of volume Ω) is

$$\frac{1}{2}\frac{1}{\Omega}\sum_{\vec{q}} \Delta n(\vec{q})\Delta v(-\vec{q}) , \qquad \text{(B5)}$$

where $\Delta v(\vec{q})$ is the Fourier transform of $\Delta v(\vec{r})$ and

$$\Delta n(\vec{q}) = \frac{\Pi_0(q)}{\tilde{\epsilon}(q)}\Delta v(\vec{q}) \qquad \text{(B6)}$$

is the linear response of the density. Expressions for the noninteracting response function Π_0 and dielectric function $\tilde{\epsilon}$ in the local density approximation are given elsewhere.[24]

The square of the vibration frequency has classical Madelung and electronic terms:

$$\omega^2 = \omega_{\mathrm{cl}}^2 + \omega_e^2 . \qquad \text{(B7)}$$

In our model, (B5) and (B6) imply that

$$\omega_e^2 = \frac{\Omega_0}{M\pi d}\int_0^\infty dk \frac{\Pi_0(k)}{\tilde{\epsilon}(k)} |V(k)|^2 , \qquad \text{(B8)}$$

where Ω_0 is the volume per ion and

$$V(k) = \frac{4\pi e^2 \bar{n} d}{k}\cos k r_c . \qquad \text{(B9)}$$

[1] F. Jona, D. Sondericker, and P. M. Marcus, J. Phys. C 13, L155 (1980).
[2] A. Bianconi and R. Z. Bachrach, Phys. Rev. Lett. 19, 104 (1979).
[3] J. P. Perdew and R. Monnier, J. Phys. F 10, L287 (1980).
[4] G. P. Alldredge and L. Kleinman, J. Phys. F 4, L207 (1974).
[5] G. Paasch and M. Hietschold, Phys. Status Solidi B 83, 209 (1977).
[6] M. Hietschold, G. Paasch, and I. Bartoš, Phys. Status Solidi B 101, 239 (1980).
[7] U. Landman, R. N. Hill, and M. Mostoller, Phys. Rev. B 21, 448 (1980).
[8] R. Monnier and J. P. Perdew, Phys. Rev. B 17, 2595 (1978).
[9] J. P. Perdew and A. Zunger, Phys. Rev. B 23, 5048 (1981).
[10] D. C. Langreth and J. P. Perdew, Phys. Rev. B 15, 2884 (1977); 21, 5469 (1980).
[11] S. H. Vosko, R. Taylor, and G. H. Keech, Can. J. Phys. 43, 1187 (1965).
[12] R. Monnier, J. P. Perdew, D. C. Langreth, and J. W. Wilkins, Phys. Rev. B 18, 656 (1978).
[13] G. Jezequel, Phys. Rev. Lett. 45, 1963 (1980).
[14] N. D. Lang and W. Kohn, Phys. Rev. B 1, 4555 (1970).
[15] G. Paasch and M. Hietschold, Phys. Status Solidi B 67, 743 (1975); M. Hietschold, G. Paasch, and P. Ziesche, Phys. Status Solid B 70, 653 (1975).
[16] M. W. Finnis and V. Heine, J. Phys. F 4, L37 (1974).
[17] C. Tejedor and F. Flores, J. Phys. F 6, 1647 (1976).
[18] R. S. Nelson, D. J. Mazey, and R. S. Barnes, Philos. Mag. 11, 91 (1965).
[19] J. H. Rose and J. F. Dobson, Solid State Commun. 37, 91 (1981).
[20] V. Sahni, J. P. Perdew, and J. Gruenebaum, Phys. Rev. B 23, 6512 (1981).
[21] K.-P. Bohnen and S. C. Ying, Phys. Rev. B 22, 1806 (1980).
[22] G. P. Alldredge, in *Computer Simulation for Materials Applications, Nuclear Metallurgy,* edited by R. J. Arsenault, J. R. Beeler, Jr., and J. A. Simmons (Natl. Bur. Stands, Washington, D.C., 1976), Vol. 20, p. 582.
[23] K.-P. Bohnen (unpublished).
[24] J. P. Perdew and T. Datta, Phys. Status Solidi B 102, 283 (1980).
[25] J. L. Yarnell, J. L. Warren, and S. H. Koenig, in *Lattice Dynamics,* edited by R. F. Wallis (Pergamon, New York, 1965), p. 57.